Time-resolved study of energy-transfer collisions in a sample of cold rubidium atoms

R. A. D. S. Zanon,* K. M. F. Magalhães, A. L. de Oliveira,† and L. G. Marcassa
Instituto de Física de São Carlos, Universidade de São Paulo, Caixa Postal 369, 13560-970, São Carlos, São Paulo, Brazil
(Received 4 May 2000; revised manuscript received 5 March 2001; published 10 January 2002)

In this work we probe the time dynamics of a collisional process involving energy transfer in a sample of cold Rydberg atoms produced in a rubidium magneto-optical trap. The $31S_{1/2}$ population, produced by collisions between the $29P_{3/2}$ and $29P_{1/2,3/2}$ states, is monitored as a function of time through the pulsed-field ionization technique. The experimental results were compared with a dynamic model based on a two-body interaction using a $1/R^5$ potential. The model can reproduce well the time evolution of this collisional process. We are also able to explain the large electric-field range over which inelastic collisions are possible based on the existence of thresholds where collisional channels open and close.

DOI: 10.1103/PhysRevA.65.023405 PACS number(s): 32.80.Pj, 33.80.Ps, 34.50.Rk, 34.80.Qb

Collisions of Rydberg atoms have been studied in depth both theoretically and experimentally in recent decades [1]. Their large size and low binding energies make Rydberg atoms irresistible for collisional experiments. Interactions involving Rydberg atoms can be divided into two categories [1]: (i) short-range-interaction collisions, which involve a Rydberg atom and some neutral partner (either another atom or a molecule); (ii) long-range-interaction collisions, which may involve a Rydberg atom and either a charged particle or another Rydberg atom, both processes having large collisional cross section. One well-known process involving two Rydberg atoms is called energy-transfer collision, which has the unique characteristic that its cross section can be tuned by a static electric field using the Stark effect. This can be either enhanced or suppressed by tuning the static electric field.

This collisional process has been studied for several alkalis, using thermal atoms deriving from an atomic beam [2]. This thermal source, however, has some intrinsic limitations. (i) The velocity distribution of the atomic beam is very large; therefore, many velocity classes contribute to the collisional rate. (ii) Due to the large velocities, it is very difficult to observe the time evolution of the process. With the advent of the magneto-optical trap (MOT), cold samples of atoms, which are naturally Doppler-free, can now be produced very easily [3]. Several groups have recently succeeded in producing cold samples of Rydberg atoms in a MOT and in observing collisional processes [4–6]. This achievement has opened up an entirely new field, allowing several different experiments to be carried out, e.g., collisions [4,5,7], high-resolution microwave spectroscopy [8], lifetime measurements [9], and cold plasma [10]. This paper reports, on a time-resolved experiment of energy-transfer collisions using cold Rydberg atoms in a MOT. The experimental results are compared with a model that takes into account the dynamics of the collisional process under the influence of a $1/R^5$ potential and radiative decay. This model is able to reproduce well our experimental data and may provide an alternative explanation for the broad energy width observed in our experiment and in Refs. [4,5], without invoking many-body effects. In fact, our model, suggests that the large energy width observed by us is coming from the fact that the collision is only energetically possible within some static electric-field range. The following collisional process was studied in our experiment:

$$\mathrm{Rb}(29P_{3/2}) + \mathrm{Rb}(29P_J) \rightarrow \mathrm{Rb}(29S_{1/2}) + \mathrm{Rb}(31S_{1/2}), \quad (1)$$

where J can be either 1/2 or 3/2. In Fig. 1, we show the energy difference between the entrance and exit collisional channels as a function of the applied static electric field. The collision is energetically accessible for $J=1/2$ between 890 V/cm and 903 V/cm (full line) and for $J=3/2$ between 857 V/cm and 915 V/cm (dashed line). The binding energy of the $29P_{3/2}$ state as a function of the static electric field is also shown in Fig. 1 (dotted line). We should point out that the binding-energy curve for the $29P_{1/2}$ state is parallel to the

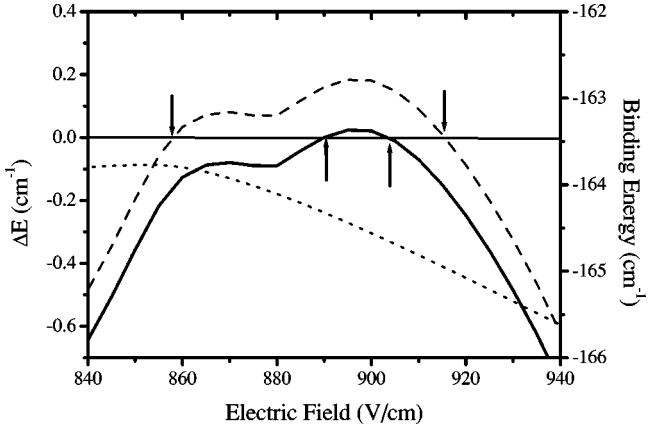

FIG. 1. Energy difference (ΔE) between the Rb $29P_{1/2}$ + Rb $29P_J$ and Rb $29S_{1/2}$ + Rb $31S_{1/2}$ atomic levels as a function of the electric field. The collision is energetically accessible for $J=1/2$ between 890 V/cm and 903 V/cm (full line) and for $J=3/2$ between 855 V/cm and 913 V/cm (dashed line). The binding energy of the $29P_{3/2}$ state as a function of the static electric field is also shown (dotted line). The arrows indicate where the processes are energetically accessible.

*Permanent address: Instituto de Química de São Carlos, Universidade de São Paulo and Universidade do Estado de Santa Catarina.

†Permanent address: Departamento de Física, Universidade Federal de São Carlos and Universidade do Estado de Santa Catarina.

$29P_{3/2}$ state. This curve is important for the understanding of the electric-field dependence of the studied collisional process because for a given laser frequency, which excites the Rydberg state, the pulsed laser detuning will vary as the electric field is scanned. This variable detuning will change the atomic population in the $29P$ Rydberg state. We should point out that collisions involving two atoms in the $29P_{1/2}$ state is only allowed in an electric field of about 600 V/cm, and it will not be considered here. All the curves were obtained using Ref. [11]. The long-range interaction between the two $29P$ Rydberg atoms is given by a potential $V=C_5/R^5$, where C_5 is a constant coefficient and R is the atomic internuclear distance. This potential may by calculated using perturbation theory. The perturbation term in the electronic Hamiltonian of two interacting atoms is given by the Coulomb interaction between the charge distributions of the atoms. Then the C_5/R^5 term is obtained from the first-order correction perturbation theory [12].

Our MOT operates in a closed stainless steel vapor cell. The Rb vapor from a reservoir maintained at $-20\,^{\circ}\mathrm{C}$ effuses through a valve into the main chamber kept at a background pressure of 10^{-10} Torr. Three mutually orthogonal, retroreflected laser beams from an injection locked diode laser tuned to 5 MHz to the red of the atomic $5S_{1/2}(F=3) \rightarrow 5P_{3/2}(F'=4)$ transition, intersect at the center of the quadrapole magnetic field generated by a pair of anti-Helmholtz coils. The magnetic field coils are located outside the chamber and produce an axial-field gradient of about 10 Gauss/cm near the center. A diode laser tuned to the $5S_{1/2}(F=2) \rightarrow 5P_{3/2}(F'=3)$ transition works as a repumper. The total trap intensity is about 50 $\mathrm{mW/cm^2}$. This configuration of static magnetic field and light field, with appropriate laser polarization, creates an environment that traps and cools atoms to about 100 μK. The number of trapped atoms is measured by imaging their fluorescence onto a calibrated photomultiplier tube (PMT) and the volume of the cloud can be derived from pictures taken with a camera charge-coupled device. These two values are used to calculate the atomic density. Under our conditions, the total number of atoms was $N_{\mathrm{Rb}} \sim 5\times10^7$ and the density was about 2×10^{10} atoms/$\mathrm{cm^3}$. We excite the Rb atoms from the $5P_{3/2}$ state to the $29P$ state using a homemade pulsed dye laser (1 mJ/pulse, 4 ns, repetition rate 20 Hz, $\lambda \sim 480$ nm) pumped by the third harmonic of a Nd:YAG laser. The dye laser has a linewidth of about 0.8 $\mathrm{cm^{-1}}$, which was measured using a fixed Fabry-Perot etalon [13]. Both fine-structure levels are populated by the pulsed laser (the energy splitting between the levels is 0.156 $\mathrm{cm^{-1}}$). The population ratio between the P levels was estimated to be about $P_{1/2}/P_{3/2} \cong 0.5$ by comparing the ion signal obtained for the process $\mathrm{Rb}(29P_{3/2})+\mathrm{Rb}(29P_{3/2})$ (at 885 V/cm) with the process $\mathrm{Rb}\,29P_{1/2}+\mathrm{Rb}\,29P_{1/2}$ (at 600 V/cm). Note that this ratio depends on the population distribution in the hyperfine levels of the $5P_{3/2}$ state. The cold cloud of atoms is formed between two metal grids, separated from each other by 3.2 cm. To one of these grids we apply a 1 μs rise-time high-voltage pulse in order to ionize the Rydberg atoms. The amplitude of the pulsed field is 430 V/cm, which allows by itself the ionization from the $31S_{1/2}$ state only. To the other grid a static voltage is applied during the whole experiment. These voltages were applied with opposite signs to the two grids so that the electric fields add, and it can be varied from 840 V/cm to 940 V/cm. The ions are detected by a channeltron particle multiplier placed behind this second grid and selected by a gated counter. By varying the delay between the optical excitation and the high-voltage pulse allows one to observe the time evolution of the $31S_{1/2}$ state population.

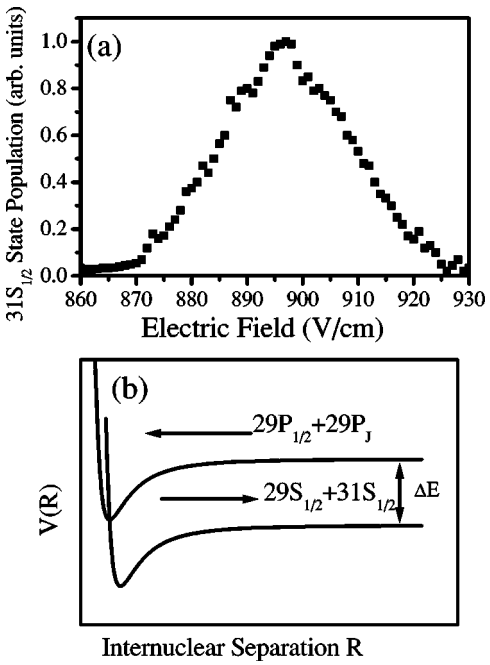

FIG. 2. (a) Population of the $31S_{1/2}$ level produced by collisions between $\mathrm{Rb}\,29P_{1/2}+\mathrm{Rb}\,29P_J$ as a function of the static electric field (delay time of 2 μs); the pulsed laser frequency was set at -164.5 $\mathrm{cm^{-1}}$ below the Rb ionization limit; (b) schematic attractive potential curves for the $\mathrm{Rb}\,29P_{1/2}+\mathrm{Rb}\,29P_J \rightarrow \mathrm{Rb}\,29S_{1/2}+\mathrm{Rb}\,31S_{1/2}$ collision. The position of the crossing is not known due to the lack of information on the potentials for Rydberg atoms.

In Fig. 2(a) we show the $31S_{1/2}$ state population as a function of the static electric field, for a delay time of 2 μs and the pulsed laser frequency kept fixed at -164.5 $\mathrm{cm^{-1}}$, below the Rb ionization limit. From Fig. 1, we conclude that the $31S_{1/2}$ population may be originated from collisions involving both the energetically accessible channels ($J=1/2$ and $J=3/2$). The shape of this ion signal is determined by the region where the collision process is allowed ($\Delta E>0$), by the population ratio between $J=1/2$ and $J=3/2$, by the pulsed laser frequency, and by its linewidth. We should point out that modeling of such line shape would be very interesting. However, this is very difficult to implement due to its dependence on several parameters. This modeling would be much easier to be implemented in collisions taking place at lower static electric fields, where the atomic population of the entrance collisional channel does not vary as a function of the dc field. One may notice that there is a discrepancy between the data of Fig. 2(a) and the calculation shown in Fig. 1. The entire ion signal is about 10 V/cm higher in electric field for the data than the region in Fig. 1 where the $29P_{3/2}+29P_{3/2}$ collision channel is above threshold. This

fact may be due to the accuracy of our high-voltage power supply, which was about 2%, responsible for the static electric field. We have carried out the experiment for different values of static electric field (where $\Delta E>0$), and all of them presented the same time evolution. We also checked for a density dependence and observed that the amplitude of the signal is proportional to n^2, but its time behavior does not depend on the atomic density (the Rydberg atomic density varied from 10^7 to 10^9 atoms/cm^3).

To explain the above results, the semiclassical model proposed by Gallagher and Pritchard [14] was adapted to the present case. In this adapted model, there are two attractive potential curves, one that connects adiabatically to the $29P_{3/2}+29P_J$ state and another that connects to the $29S_{1/2}+31S_{1/2}$ state. The latter presents lower energy than the former, as schematically shown in Fig. 2(b). We consider that these curves cross each other at a very short range. The position of the crossing is not known due to the lack of knowledge about the potentials for Rydberg atoms. We also assume that at $t=0$ the laser pulse excites the atoms to the $29P_{3/2}+29P_J$ Rydberg potential for all possible internuclear separations (from $R=0$ to $R\rightarrow\infty$). Once they are under the influence of this potential, the colliding atoms will accelerate towards each other until they reach a short internuclear separation. In this region, the atomic pair may change potential, completing the collision process in the $29S_{1/2}+31S_{1/2}$ state, when the $31S_{1/2}$ population is detected. To calculate the time evolution of the $31S_{1/2}$ state population, one has to know the $29P_{3/2}+29P_J$ potential curve. However, this information is not available in the literature; thus, we will assume a $1/R^5$ potential for our model as explained before. The long-range potential for the $29S_{1/2}+31S_{1/2}$ state can be expressed as $1/R^6$, but we will consider it flat in this model.

The first step in the model is to calculate the density of colliding pairs (ΔN) present at an internuclear separation between R_0 and R_0+dR_0. This can be expressed in terms of R_0 as

$$\Delta N=\frac{4\pi}{2}n^2R_0^2dR_0, \tag{2}$$

where n is the Rydberg atomic density. These pairs may reach short-range separation, where the potential change takes place, between t and $t+dt$. If one considers a pure $-C_5/R^5$ potential, one can calculate this time (t) necessary for a pair to go from $R=R_0$ to $R=0$ with an initial velocity equal to zero, which is given by

$$t=\frac{B(1/2,7/10)}{5}\left(\frac{\mu R_0^7}{2C_5}\right)^{1/2}, \tag{3}$$

where μ is the reduced mass and B is the beta function. Therefore, Eq. (2) can be rewritten as

$$\Delta N=\frac{4\pi}{7}n^2\left(\frac{2C_5}{\mu}\right)^{3/7}\left(\frac{5}{B(1/2,7/10)}\right)^{6/7}t^{-1/7}dt. \tag{4}$$

Next one takes into account the probability of the colliding pair to survive spontaneous decay and to reach the short range. At short range, the pair has a probability q to change the potential curve. Therefore, the probability (P_r) that a pair will survive spontaneous decay and change its potential is given by

$$P_r=e^{-2t/\tau}q, \tag{5}$$

where τ is the lifetime of the initial state ($29P$), while the factor of 2 accounts for the fact that either of the two atoms may decay. This probability (P_r) accounts only for half a vibrational cycle in this potential. To account for several vibrations of the pair in the potential before the pair decays or changes potential, one has to rewrite Eq. (5) as [14]

$$P_r=qe^{-2t/\tau}+qe^{-2t/\tau}e^{-4t/\tau}(1-q)+qe^{-2t/\tau}e^{-4t/\tau}\times(1-q)e^{-4t/\tau}(1-q)+\cdots, \tag{6}$$

$$P_r=\frac{e^{-2t/\tau}q}{1-(1-q)e^{-4t/\tau}}. \tag{7}$$

We should point out that the multiple oscillations may not be completely correct for this situation. The exciting laser has a much larger linewidth than both the kinetic energy of the atoms and the detuning from the Rydberg state. In this situation there is no frequency selectivity that requires the atoms to be bound. Therefore, some fraction of the atoms should not undergo multiple oscillations but rather just a single pass through the excited attractive potential. However, if we consider only the first oscillation we do not observe a considerable change in the final result. Nevertheless, this remains to be investigated in a future experiment.

Finally, to account for the atomic pairs that change potential for $t<\tau_1$, one must integrate over time from $t=0$ to $t=\tau_1$. To account for the fraction of the population that changed potential at time t and survived spontaneous decay in the $31S_{1/2}$ state until $t=\tau_1$ we add the term $e^{-(\tau_1-t)/\tau'}$. Therefore, the total number of pairs in the $29S_{1/2}+31S_{1/2}$ potential is given by

$$N(\tau_1)=\frac{4\pi}{7}n^2\left(\frac{2C_5}{\mu}\right)^{3/7}\left(\frac{5}{B(1/2,7/10)}\right)^{6/7}\times\int_0^{\tau_1}t^{-1/7}\frac{e^{-2t/\tau}q}{1-(1-q)e^{-4t/\tau}}\exp[-(\tau_1-t)/\tau']dt, \tag{8}$$

where τ' is the lifetime of the $31S_{1/2}$ state. Equation (8) allows one to predict the behavior of the atomic population as a function of time. For short times, the number of pairs that reach short internuclear separation is small; hence, the population in the $31S_{1/2}$ state is also small. In time, the pairs at longer internuclear separations reach the short range and change their potential, and the population in $31S_{1/2}$ state increases. For longer times, spontaneous decay is responsible for the decrease in the population of the $29P$ and $31S$ states. Figure 3 shows the theoretical curve (solid line) predicted by Eq. (8) together with the experimental results. For this curve, theoretical values were used for the $29P$ and $31S$ lifetimes

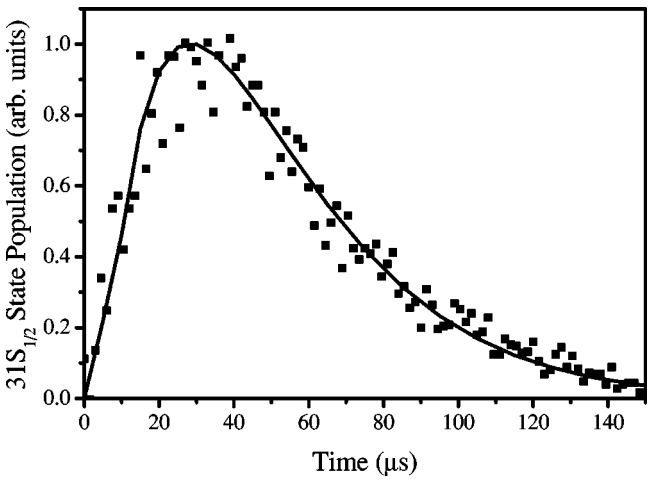

FIG. 3. Comparison between the experimental result (■) and the model prediction (full line) for the time evolution of the $31S_{1/2}$ population.

($\tau_{29P}=44$ μs and $\tau_{31S}=24$ μs) [1]. The lifetimes of the $29P$ and $31S$ states were also measured, using the cold sample; the results agree well with the theoretical values and will be published elsewhere. The theoretical prediction presents a peak at $t=29$ μs and the experiment, at $t=33$ μs (Fig. 3). The ratio signal to noise around the peak is low to draw precise conclusions about such deviation, however, we believe that this small difference may be an evidence that the potential presents repulsive terms of higher order. In such potential, the atomic pair would be under a weaker acceleration than in the $1/R^5$ potential, therefore, the atomic pairs would need more time to reach the short range and the curve peak would move to longer times. The higher-order repulsive terms may come from the interaction between the attractive and repulsive potential curves of the different collisional channels ($29P_{3/2}+29P_{3/2}$, $29P_{1/2}+29P_{3/2}$, and $29P_{1/2}+29P_{1/2}$), which was not considered here. The only free parameter in the model presented here is the probability q of changing potential; in the case of Fig. 3, the best fit was obtained using $q=0.5$. This parameter may be calculated using the Landau-Zener model [15]. To calculate q one has to know precisely the potentials at short range in order to calculate the coupling between the molecular potentials (Ω), the atomic velocity at the crossing (v), and the slope of the difference between the potentials (dV/dR). However, this information is not available in the literature. Nevertheless, the fitted value for q is consistent with this model, which predicts $0 \leqslant q \leqslant 0.5$.

It is important to point out that we are comparing experimental results, which may involve collisions with both $J's$, with a model that just considers one channel. To evaluate this effect in the experimental results, we have carried out the same experiment for different population distributions in the $29P$ states. For an electric field of 897 V/cm, we have not observed any appreciable variation in the time evolution of the $31S_{1/2}$ state population as a function of the population distribution. Therefore, our results indicate that this collision process may be insensitive to fine-structure levels. However, more experiments are underway to verify this.

In summary, we measured the time evolution of the energy-transfer collision involving cold Rydberg atoms in a sample of trapped ^{85}Rb atoms. The experimental results were compared with a dynamic model, based on a two-body interaction, and a good agreement was observed. The model can reproduce the time evolution of the collisional process. We were also able to explain the large energy width observed in our experiment as coming from the fact that the collision $29P_{3/2}+29P_j$ is only energetically possible within some static electric-field range. Basically, we had shown that there are thresholds where collisional channels open and close. New experiments involving resonances at lower fields to study such collisions, varying the principal quantum number, are currently being carried out.

This work received financial support from FAPESP (Fundação de Amparo à Pesquisa do Estado de São Paulo), PRONEX (Programa de Núcleos de Excelência em Óptica Básica e Aplicada), and FINEP (Financiadora de Estudos e Projetos). The authors thank L. Misoguti and J. Weiner for technical help, and R. Napolitano for critical reading. We also thank D. Kleppner for the software to calculate the Stark effect. This work was carried out at the Center for Research in Optics and Photonics—CePOF.

[1] T. F. Gallagher, *Rydberg Atoms* (Cambridge University Press, Cambridge, 1994).
[2] K. A. Safinya, J. F. Delpech, F. Gounand, W. Sandnern, and T. F. Gallagher, Phys. Rev. Lett. **47**, 405 (1981); D. S. Thomson, M. J. Renn, and T. F. Gallagher, *ibid.* **65**, 3273 (1990).
[3] C. Monroe, W. Swann, H. Robinson, and C. Wieman, Phys. Rev. Lett. **65**, 1571 (1990).
[4] I. Mourachko, D. Comparat, F. de Tomasi, A. Fioretti, P. Nosbaum, V. M. Akulin, and P. Pillet, Phys. Rev. Lett. **80**, 253 (1998).
[5] W. R. Anderson, J. R. Veale, and T. F. Gallagher, Phys. Rev. Lett. **80**, 249 (1998).
[6] S. Rolston (private communication).
[7] S. K. Dutta, D. Feldbaum, A. Walz-Flannigan, J. R. Guest, and G. Raithel, Phys. Rev. Lett. **86**, 3993 (2001).
[8] M. Weidemüller, C. Gabbanini, J. Hare, M. Gross, and S. Haroche, Opt. Commun. **101**, 341 (1993).
[9] K. M. F. Magalhães, A. L. de Oliveira, R. A. D. S. Zanon, V. S. Bagnato, and L. G. Marcassa, Opt. Commun. **184**, 385 (2000).
[10] T. C. Killian, M. J. Lim, S. Kulin, R. Dumke, S. D. Bergeson, and S. L. Rolston, Phys. Rev. Lett. **86**, 3759 (2001).
[11] M. L. Zimmerman, M. G. Littman, M. M. Kash, and D. Kleppner, Phys. Rev. A **20**, 2251 (1979).
[12] M. Marinescu, Phys. Rev. A **56**, 4764 (1997).
[13] M. G. Littman and H. J. Metcalf, Appl. Opt. **17**, 2224 (1978).
[14] A. Gallagher and D. E. Pritchard, Phys. Rev. Lett. **63**, 957 (1989).
[15] C. Zener, Proc. R. Soc. London, Ser. A **137**, 696 (1932).